Paper No. 226, Bull. ISET, Vol. 20, No. 1, March 1983, pp. 1–22

ESTIMATES OF SEISMIC HAZARD IN NORTHWESTERN INDIA AND NEIGHBOURHOOD

K. N. KHATTRI[1], A. M. ROGERS[2] AND D. M. PERKINS[2]

INTRODUCTION

The entire northern India, along the Himalaya mountains and the frontal Indo-Ganga plains, is prone to occasional destructive earthquakes. Historical records show that in these earthquakes more than sixty thousand lives were lost as well as causing immeasureable misery to the survivors (Oldham, 1883, 1899, 1926; Middlemiss, 1910; Milne, 1911; Auden and Ghosh, 1934; Gee 1934; Rao, 1953).

The shadows of a possible occurrence of a major earthquake loom large in these regions because the physical processes causing the catastrophic events continue on a geological time scale. Although scientists are presently trying to understand and model the processes that lead up to the fracturing of rocks and causing earthquakes so that the earthquakes could possibly be precisely predicted, the goal still appears to be a distant one. However, so far as saving of civil works is concerned, an earthquake prediction has somewhat limited utility because the efforts to strengthen structures would probably be directed to only the most important ones. On the other hand if information regarding the expected damaging earthquakes in an area is available, the structures could be designed to withstand damage, should such an earthquake occur during the life time of the utility of the structure. Owing to the uncertainties in the time of occurence, the location and the magnitude of earthquakes, they can be considered as a random process. Accordingly, the estimates of the seismic hazard can suitably be made on the basis of a statistical model of earthquake occurence.

The early attempts to provide estimates of seismic hazard in the area of concern consisted of specifying maximum expected intensity of shaking in terms of modified Mercalli intensity (MMI) scale specifying the maximum magnitude of an earthquake or stating the peak acceleration in various zones (e.g., West, 1936; Tandon, 1956; Auden, 1959; Mithal and Srivastava, 1959; Krishna, 1959; Guha, 1962; Gaur and Chauhan, 1968; ISI, 1975). The utility of such

[1]Earth Sciences Department, Roorkee University, Roorkee, UP 247667, INDIA.
[2]U.S. Geological Survey, Denver Federal Center, Box 25046 MS 966, Denver, Colorado 80225, USA.

seismic hazard estimates is circumscribed by the lack of information regarding the probability of experiencing the specified ground shaking in a given period of time. Recent investigations have tackled this problem from a stochastic view point and have produced seismic hazard maps of India that contain information on the probability of occurrence of a given peak ground motion in a specified time interval (Basu and Nigam, 1977, 1978; Hattori, 1979; Kaila and Rao, 1979; Basu and Srivastava, 1981). The above investigators have not classified the seismic areas of India into seismic source zones that are governed by homogeneous or quasihomogeneous seismotectonic regimes. It is crucial to do so in order to obtain appropriate estimation of seismic hazard. In the present analysis the historical seismicity of the Indian region is classified according to the seismotectonic units which are considered to be governed by the same or similar geotectonic processes (Khattri et al. 1983). A point random model with Poisson distribution has been assumed to represent the occurrence of earthquakes. A point of departure from the previous investigations is the use of a different distance attenuation law in the present investigation. Three seismic hazard maps have been prepared with exposure periods of fifty, one hundred and two hundred years respectively. Contours of peak ground acceleration having 10% probability of exceedence in the exposure period have been drawn. The mapped hazard principally relates to the damage risk due to vibrations. Two additional sources of seismic damage are the associated damages due to faulting and rock slide which have not been estimated in the present investigation.

SEISMOTECTONIC SETTING

The area under consideration can be divided into two physiographic divisions. The northern division consists of the Himalaya mountains, and the contiguous southern part is composed of the flat alluvial tracts of the Sindhu-Ganga vally. Major thrust systems consisting of the Main Boundary Thrust (MBT), the Krol thrust, the Main Central Thrust (MCT) and the Indus Suture Thrust (IST) traverse the northern mountainous division. These great thrust faults dip towards north, with the exception of the IST which dips towards south (see Figure 1) (Gansser, 1964). The historical seismicity characterizes the arcuate Himalaya mountain chain. The epicenters fall close to the MCT although they exhibit a somewhat diffused pattern (Figure 2). This is expected in view of thrust planes dipping at shallow angles, faulting on which causes earthquakes. Furthermore, the complexity of tectonics of the area would also lead to diffusion of the epicenters. A zone of epicenters is present in a part of the alluvial tract to the south. The major earthquakes have originated towards the southern edge of the zone of epicenters present in Himalaya.

The seismicity, together with the tectonic features of the area have been the basis of indentifying seismic source zones for the purpose of calculating seismic hazard. The basic notion is that a seismic source zone is considered to be a geodynamic unit undergoing deformation on account of homogeneous

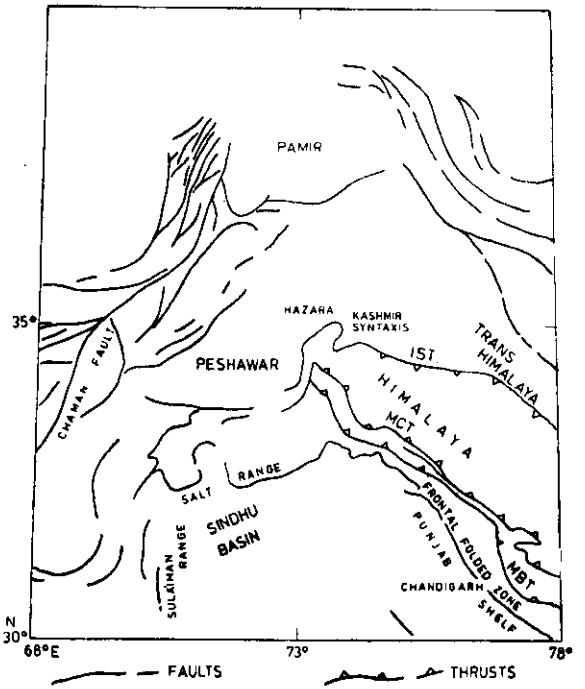

Fig. 1. The generalized tectonic features of the area. IST = Indus Suture Thrust MCT = Main Central Thrust; MBT = Main Boundary Thrust

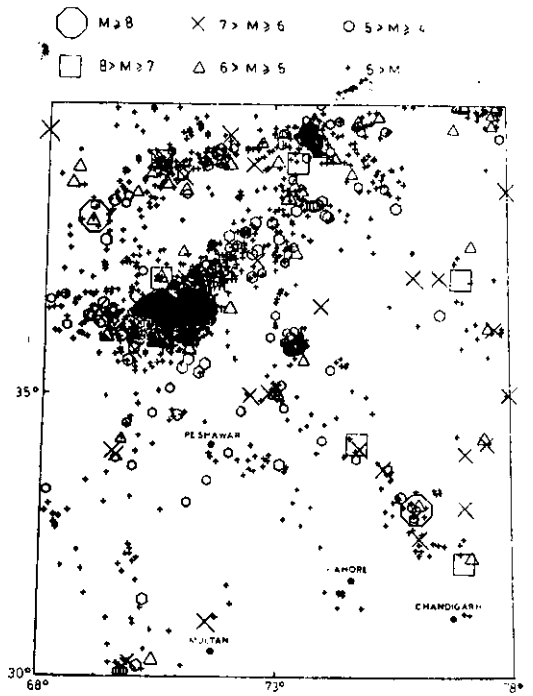

Fig. 2. The Seismicity of the area from 1900–1976

or quasihomogenous tectonic forces. Therefore the associated seismic activity will also be homogeneous or quasihomogeneous in such a source zone. The future earthquake occurrences can be expected to have the same average behaviour pattern as in the past. Accordingly the estimates of the parameters of recurrence rates of earthquakes for such source zone can be used with greater reliance for the estimates of future occurrence of earthquakes and the associated hazards. The sections of such source zones falling in the area of the present study are shown in Figure 3.

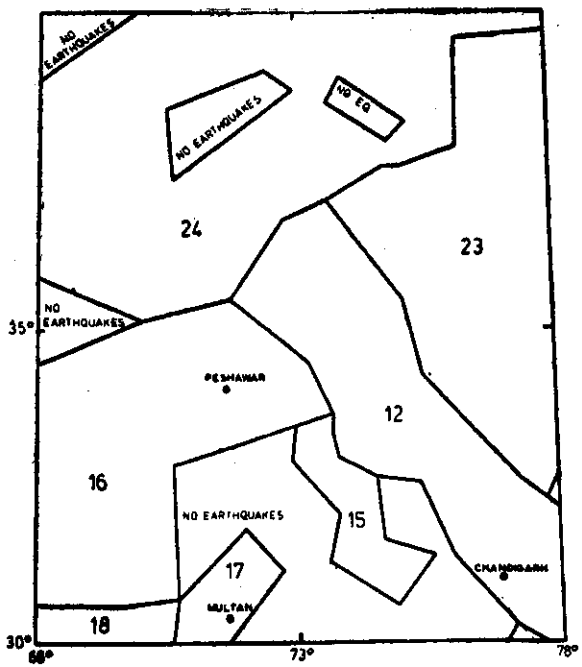

Fig. 3. The seismic source zones. The numbers identify the source zones. The areas marked as 'No Earthquakes' designate regions lying outside defined source zones, although may have isolated feeble earthquakes.

THE EARTHQUAKE SOURCE MODEL

Recurrence Relation:—The following relationship between the number of earthquakes $N_c(M)$ having magnitude equal to or greater than M occuring during a unit interval of time and in a unit area has been found to hold (Gutenberg and Richter, 1956).

$$\log_{10} N_c(M) = A - B\,M \qquad \ldots(1)$$

This is known as the cumulative magnitude recurrence relation and provides the time elapsed on an average before an earthquake with magnitude greater than a given magnitude, say M_0, will occur again. The return time is given by $1/N_c(M_0)$ years if the relation (1) has been obtained with unit interval as one year. This law is fundamental in studies concerning the estimation of seismic

hazard in earthquake prone areas and is the basis of the models for estimating seismic hazard (Cornell, 1968; Algermissen and Perkins, 1976).

The recurrence parameters A and B are usually estimated by regression analysis on historical date of seismicity. The records of historical seismicity often are incomplete and lead to errors in the estimates of A and B. This deficiency of the earthquake catalogs is time as well as magnitude dependent. For example, the records for earlier periods will be relatively more incompletely reported for smaller magnitude earthquakes because of the less sensitive and fewer seismological observatories in those periods whereas if one considers the earthquake date for the most recent twenty years, it will be complete for earthquakes in the magnitude range between 4.5 and 5.5. It is so on account of the excellent network of observatories operating during this period as well as because the return period of the earthquakes in this magnitude range is less than about fifteen years in seismically active regions. On the other hand to adequately sample the occurrence of larger magnitude events, say $M > 7$, a sufficiently long period of historical data must be considered since the return periods of such events is quite long. Moreover, in order to record a great earthquake very sensitive instruments are not required if it occurs in or nearby populated areas. This special character of historical data suggests that more reliable estimates of the recurrence parameters can be obtained if the earthquake catalog can be analysed in a moving time magnitude window (Stepp, 1973). The entire catalog of earthquakes is regrouped into magnitude ranges, say $\Delta M = 1$ unit, and in time intervals of 10 years. The average number of events per year $N_i^l(M)$, in a magnitude range of $M \pm \Delta M$ and for various time window lengths i is determined. Thus the first window consist of the recent most ten years giving

$$N_I^{10}(M) = \frac{N(M - \Delta M) - N(M + \Delta M)}{\text{Number of years } i = 10} \qquad \ldots(2)$$

Similarly the next window would consist of the recent most twenty years giving $N_I^{20}(M)$ and so on. An analysis of the series of $N_I^l(M)$ obtained as above will show the length of the time window for which $N_I(M)$ becomes stationary. This stable value will represent an estimate of the average number of earthquakes with magnitudes lying in the range $M \pm \Delta M$ that occur per year which has been compensated for incomplete reporting of earthquakes in historical catalogs. The procedure does not guarantee that compensation will be complete, however, it does provide a means to reduce the effects of incomplete reports as much as is possible. Clearly the stability of $N_I^l(M)$ would be expected to occur for very long time windows (large i) for larger events whereas for smaller events it will be for a shorter time window.

Representing the occurrence of earthquakes by the Poisson distribution, an unbiased estimate of the mean rate of earthquakes per unit time (1 year)

of a sample (historical catalog) for a given magnitude interval is (Hamilton, 1964)

$$N_I(M) = \frac{1}{r}\sum_{i=1}^{r} N_I^i(M) \qquad ...(3)$$

where $N_I^i(M)$ are r observations of the mean rates per unit time in the sub-time intervals of the above referenced sample having total duration of T years. The variance of $N_I(M)$ is given by

$$\text{Var}\quad N_I(M) = N_I(M)/T \qquad ...(4)$$

The process of the occurrence of earthquakes can be taken to be stationary, therefore, standard deviation (SD) will behave as $1/\sqrt{T}$. In Figure 4 we show the plots of the standard deviation as a function of sample length and magnitude class for source zone 12. The SD shows the expected behaviour as discussed above attaining stability in shorter time windows for the smaller earthquakes and in longer time windows for the larger magnitude earthquakes. Tangent lines with slope of $1/\sqrt{T}$ have been drawn through the stable values of SD for various magnitude ranges. These values yield the unbiased estimates of $N_I(M)$ which allow to establish the following incremental magnitude recurrence relation (Evernden, 1970).

$$\log_{10} N_I(M) = a - bM \qquad ...(5)$$

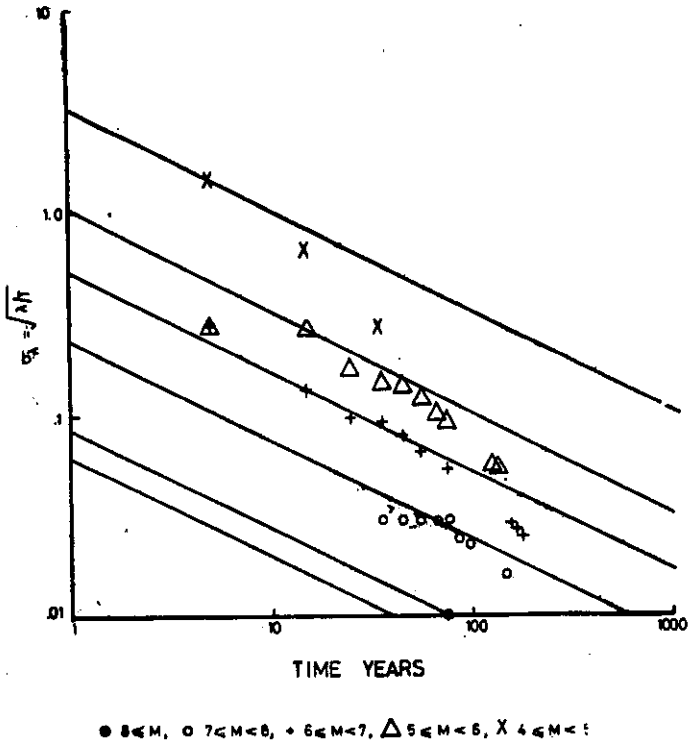

Fig. 4. The plot of standard deviation of $N_I(M)$ versus sample length and magnitude class for source zone 12.

The parameters a and b of the above relation and A and B occurring in equation (1) are connected through the following relationship.

$$B = b$$

$$A = a - b\left(\frac{M_2 - M_1}{2}\right) - \log_{10}\left(10^{-bM_1} - 10^{-bM_2}\right) \qquad \ldots(6)$$

where M_1 and M_2 are the upper and lower magnitudes of an interval.

The recurrence parameters of earthquakes for all the source zones have been established in the above manner. The values of these parameters for the source zones influencing the area under study are given in Table 1. We note that most of the source zones are large, extending beyond the perifery of Figure 3 and allow a reliable parameter estimation (Khattri, et al. 1983).

Modeling of Extreme Accelerations:—The occurrence of earthquakes in a source region can best be described statistically. The time of occurrence of the major earthquakes closely follows a Poisson process (Gardner and Knopoff, 1974). Although smaller earthquakes may depart from the Poisson model significantly, it does not cause serious error in the assessment of seismic risk as such earthquakes generate feeble ground motions. The Poisson model also assumes the distribution to be homogeneous in time, that is, the events are independent in time and are identically distributed. The distribution of earthquakes in space may be assumed to be homogeneous or non-homogeneous, depending on the spatial distribution of historical seismicity and its interrelation with the geological and tectonic factors of the source area.

The seismic hazard maps are prepared by estimating the extreme probability $F_{\max, t}(\hat{a})$ of some parameter characterizing the ground motion, e.g., acceleration, velocity or displacement. If $\hat{a}$ is the peak acceleration, then the probability that an observed acceleration a is less than or equal to the peak value, with the condition that an earthquake with magnitude M greater than some minimum magnitude of interest has occurred, is given by

$$F(\hat{a}) = P\,[a \leqslant \hat{a} \mid M \geqslant M_{\min}]$$

This probability is given by taking the ratio of the expected number of occurrences with a $\leqslant \hat{a}$ and $M \geqslant M_{\min}$ to the total expected number of occurrences of earthquakes with magnitude greater than $M_{\min}$.

For the case in which N independent earthquakes cause accelerations a_i, the cumulative distribution of the maximum acceleration of the set of N accelerations is given by

$$F_{\max}(\hat{a}) = P\,[a_1 \leqslant \hat{a}]\; P\,[a_2 \leqslant \hat{a}] \ldots P\,[a_N \leqslant \hat{a}]$$

Table 1. Earthquake Parameters for Source Zones

Source Zone	Shallow Focus Earthquakes				Deep Focus Earthquakes			
			Maximum Magnitude				Maximum Magnitude	
	a	*b*	Observed	Projected	*a*	*b*	Observed	Projected
12	5.65	−0.757	8.6	8.75	2.62	−0.437	6.75	7.0
15	3.44	−0.787	Small	7.0	—	—	—	—
16	3.73	−0.581	6.4	8.0	—	—	—	—
17	4.22	−0.787	6.5	7.0	—	—	—	—
18	3.96	−0.485	7.5	8.0	—	—	—	—
24	4.59	−0.561	8.6	8.75	5.29	−0.602	8.1	8.1

If the earthquakes are assumed to be identically distributed, the above probability takes the from

$$F_{\max}(\hat{a}) = F(\hat{a})^N \qquad \ldots(7)$$

If the number of earthquakes, N, itself is a random variable, we have

$$F_{\max}(\hat{a}) = \sum_{i=0}^{\infty} F(\hat{a})^i \, P(N = i) \qquad \ldots(8)$$

When earthquakes are represented by a Poisson process with mean occurrence rate, λ, the cumulative distribution can be written as

$$F_{\max}(\hat{a}) = \sum_{i=0}^{\infty} F(\hat{a})^i \frac{\lambda^i e^{-\lambda}}{i} \qquad \ldots(9)$$

$$= \exp\{-\lambda(1 - F(\hat{a}))\} \qquad \ldots(10)$$

The probability of recording an acceleration exceeding $\hat{a}$ is given by $[1 - F(\hat{a})]$. Therefore, the average number of earthquakes that must occur to produce such an acceleration is given by

$$RP_N(\hat{a}) = 1/[1 - F(\hat{a})] \qquad \ldots(11)$$

$RP_N(\hat{a})$ is termed the return period in terms of number of events. The more conventional return period in years is given by

$$RP_Y(\hat{a}) = RP_N(\hat{a})/\hat{N} \qquad \ldots(12)$$

where $\hat{N}$ is the expected number of earthquakes per year with $M \geqslant M_{\min}$.

Bringing the time element into consideration explicitly, if we let $\lambda = \phi t$ where ϕ is the mean rate of occurrence of earthquakes $(M \geqslant M_{\min})$ per year and t is the time interval of interest, we then have

$$F_{max,\,t}(\hat{a}) = \exp[-\phi t(1 - F(\hat{a}))], \qquad \ldots(13)$$

where we notice that

$$\phi t(1 - F(\hat{a})) = \frac{t}{RP_Y(\hat{a})} \qquad \ldots(14)$$

therefore

$$F_{\max,\,t}(\hat{a}) = e^{-t/RP_Y(\hat{a})} \qquad \ldots(15)$$

and

$$\ln\{F_{\max,\,t}(\hat{a})\} = -t/RP_Y(\hat{a}) \qquad \ldots(16)$$

The maximum acceleration with a 90 percent probability of not being exceeded in a time interval of 50 years is, therefore, given by

$$\ln (0.90) = -50/RP_Y(\hat{a}) \qquad \ldots(17)$$

which gives $RP_Y(\hat{a}) \cong 475$ years. Using 90 percent and 50 years exposure period in preparing the seismic hazard map for the region, we are in effect displaying accelerations with return period of 475 years.

The relation (15) also shows that the probability of not exceeding a particular level of acceleration $\hat{a}$ in the time interval corresponding to the return period for $\hat{a}$ is $\sim$ 37 percent and it is erroneous to take this probability as zero. Further, the return period $RP_Y(\hat{a})$ is not identical with the earthquake recurrence intervals determined for the source zones.

Distance-Attenuation laws:—Due to a lack of adequate instrumental observations of strong ground motion in India, a suitable attenuation law for the region is not available. Fortunately, a number of investigators have mapped intensity of shaking for major and medium sized earthquakes (Oldham, 1883, 1899, 1926; Middlemiss, 1910; Stuart, 1920; Gee, 1934; Auden and Ghosh, 1934; West, 1936; Rao. 1953; Gupta et al., 1969, 1972; Singh et al., 1976).

In the present analysis we have adopted an approach in which the *MM* intensity versus distance relations for the Indian region are compared with those for various parts of the United States to determine if a similar behaviour could be discovered. We then could use the acceleration versus distance law established for the matching United States zone in the area of the present study (Khattri et al., 1983).

The early studies utilized a scale different from the current Modified Mercalli Intensity scale. These reports covered the great earthquakes and contained copious descriptions of damages and also a comparison of their scales with the Rossi-Forel scale. The detailed information has enabled the present authors to approximately transform early intensity maps into the *MMI* scale. The recent earthquakes have been of comparatively moderate size, except the great 1950 Assam earthquake, and the intensity maps for them have been prepared using the *MMI* scale. The intensity distance curves for the earthquakes are shown in Figure 5. The earthquake parameters are given in Table 2.

Figure 5 shows the familiar series of intensity attenuation curves whose level is dependent on the magnitude of the earthquake. It is apparent that the two great Assam earthquakes were the largest in the region. The MM intensities of XI were recorded at considerable distances. But they seem to

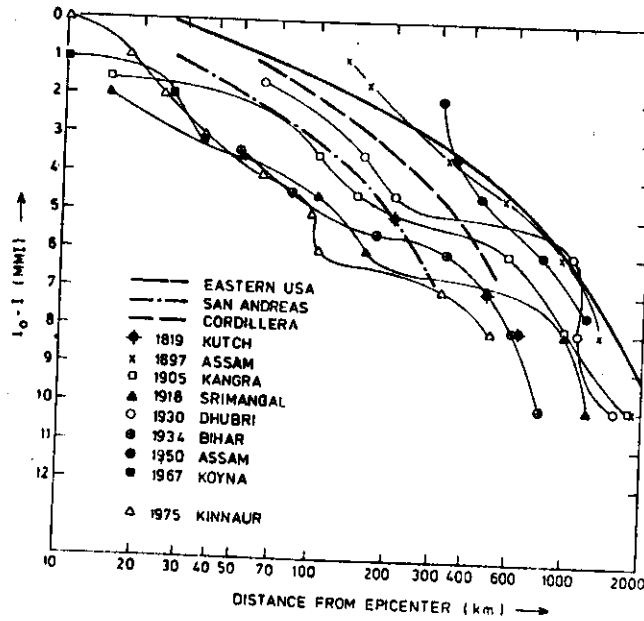

Fig. 5. Intensity-distance attenuation curves for large Indian earthquakes. The average curves for three regions of United States are also shown

Table 2. List of Large Earthquakes for which Intensity Data are used

Region	Year	Magnitude	Reference
Kutch	1819	8	Oldham (1926)
Assam	1897	8.7	Oldham (1899)
Kangra	1905	8.4	Middlemiss (1910)
Srimangal	1918	7.6	Stuart (1920)
Dhubri	1930	7.1	Gee (1934)
Bihar	1934	8.4	Auden and Ghosh (1934)
Assam	1950	8.7	Rao (1953)
Koyna	1967	6.4	Gupta et al. (1969)
Kinnaur	1975	6.8	Singh et at. (1976)

attenuate quickly thereafter. One may wonder if an overestimation could have been made here. On the other hand, the epicentral area of the 1897 earthquake consists of crystalline rocks known as the Shillong massif, and is under a considerable compressive stress due to the vice-like convergence of plates from the north and southeast. Thus, the high accelerations generated would propagate far without much attenuation due to internal friction. Once

the energy entered the thick sedimentary formations which are deposited on the flanks of this massif, there would be rapid loss, giving rise to the observed phenomenon. The attenuation relation for the eastern United States (Howell and Schultz, 1975) is also drawn in the same figure. It is noticed that this curve describes the observed curves for the great Assam earthquakes for distances beyond 150 km fairly well. At shorter distances, however, the curve for the eastern United States predicts smaller intensities than observed in Assam. The curve seems to describe the attenuation rate fairly well at the shorter distances also for the remaining Indian earthquakes. Therefore there seems to be an adequate similarity in the intensity attenuation behaviour between the Indian subcontinent and the eastern United States. There may be a difference in the attenuation behaviour of the Assam area at distances less than 100 km for the very great earthquakes where the attenuation rate of intensity appears to be lower as compared to the rate in the United States. The intensity attenuation curves for the Cordilleran and San Andreas areas of the United States are also shown in the figure. The attenuation rate is appreciably higher for the above areas as compared to the Indian regions. In view of the above similarity of attenuation behaviour between the eastern United States and the Indian region, we have selected the acceleration-distance curves developed for the eastern United States (See Figure 6) by Algermissen and Perkins (1976) for the seismic hazard analysis in India.

A major variable affecting surface ground motion distribution is the focal depth of the earthquake. The depth of focus effects the epicentral intensity as well as its attenuation with increasing epicentral distance. A number of workers have given attention to this problem and relation-ships between intensity, epicentral distance and focal depth have been proposed (e.g., Gutenberg and Richter, 1942; Shebalin, 1959; Medvedev, 1959). Unfortunately, information on intensity for deep focus earthquakes for the Indian region is scarce.

In the absence of firm theoretical analysis, heuristic rationale has been developed to derive acceleration—distance attenuation curves for deep focus earthquakes from the curves for surface focus earthquakes of Figure 6. A consideration that went into the analysis was to produce conservative estimates of the seismic hazard in the region. Therefore, all the earthquakes with depth of focus greater than 70 km were assigned a virtual depth of 100 km. The faults for the earthquakes were allowed to propagate upwards towards the surface to give the effective depth for the event as (100-fault lengths) km. The fault lengths were estimated using a relationship between magnitude and fault length given by Bonilla and Buchanan (1970). Using the effective depth, source site hypocentral distances were calculated corresponding to various epicentral distances. The acceleration values were read off the graphs of Figure 6 corresponding to the calculated hypocentral distances and replotted at the coresponding epicentral distances to produce the desired acceleration-epicentral distance attenuation curves shown in Figure 7.

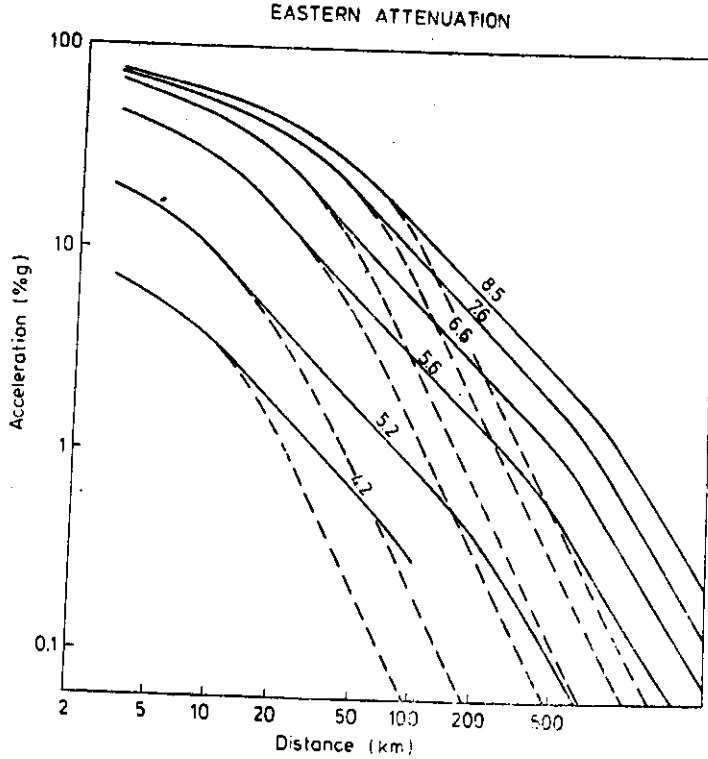

Fig. 6. Acceleration-distance attenuation curves derived for eastern United States (after Algermissen and Perkins, 1976)

These curves show the expected behavior, viz., a slow decay of ground motion near the epicenter and a fall off rate comparable to that for shallow focus events at larger distances. The seismic risk analysis for deep focus events has been computed using the above curves.

The procedure of estimating the earthquake hazard at a site consists of the following steps.

1. Estimate future occurrence of earthquakes in exposure period on the basis of recurrence relation.
2. Distribute these events over grid points drawn in the earthquake source zone.
3. Numerically calculate the frequency of occurrence of accelerations in various discrete ranges over the grid points due to sources also distributed over grid points within the earthquake source zones (as in (2) above).
4. Calculate the extreme probability $F_{\max, t}(\hat{a})$ of peak ground acceleration for exposure time t at each of the grid points. These values are contoured to prepare the seismic hazard map.

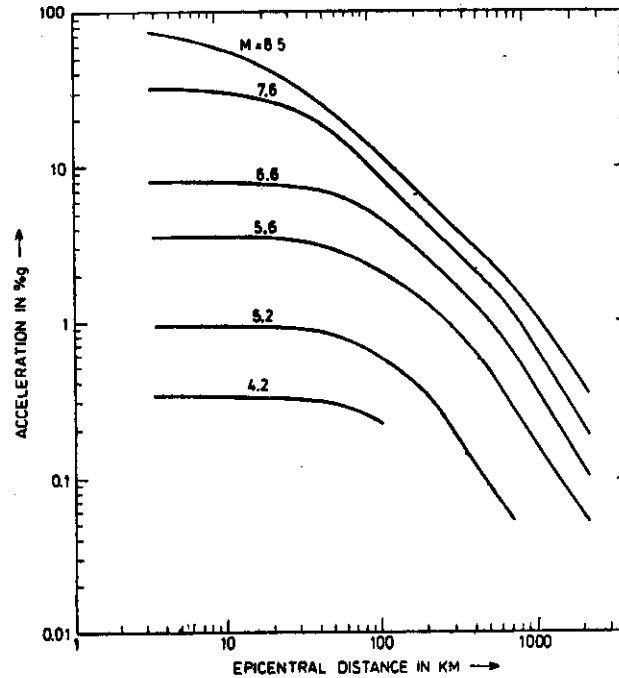

Fig. 7. Acceleration-distance attenuation curves derived for deeper focus (H>70 km) earthquakes

SEISMIC HAZARD MAPS

The seismic hazard maps are shown in Figures 8 (a), (b) and (c). The contours mainly follow the seismic source zones. The fifty years exposure period map displays a highest value of peak acceleration of 57% *g* in the southwest corner of the map in the region lying west of Multan. The highest peak acceleration estimated in the Himalaya region is 35% *g*. The area lying in between these two zones of higher seismic risk displays value of 5 to 7% *g* peak ground acceleration, the lowest values being where there is no seismic source zone. The one hundred and the two hundred year exposure period maps display similar pattern of contours as the fifty year exposure period map does. The maximum values of the peak acceleration obtained for the one hundred year exposure period are 45% *g* in the Himalaya and 66% *g* in the south-west corner. Similarly the maximum estimated peak acceleration values for the two hundred year period are 55% *g* in the Himalaya and 70% *g* in the south-west corner of the map. A common feature of these maps is that the drop in peak acceleration values takes place rapidly near the boundaries of the source zones with no source areas. The rate of drop is faster for longer exposure period estimate. This phenomenon is to be expected since near the borders of the source zones with non-source areas there is a rapid change in the number of earthquakes contributing to peak

ground acceleration at an observation point as well a the nature of the attenuation of peak ground acceleration with distance rapidly reduces the effects of the distant earthquakes.

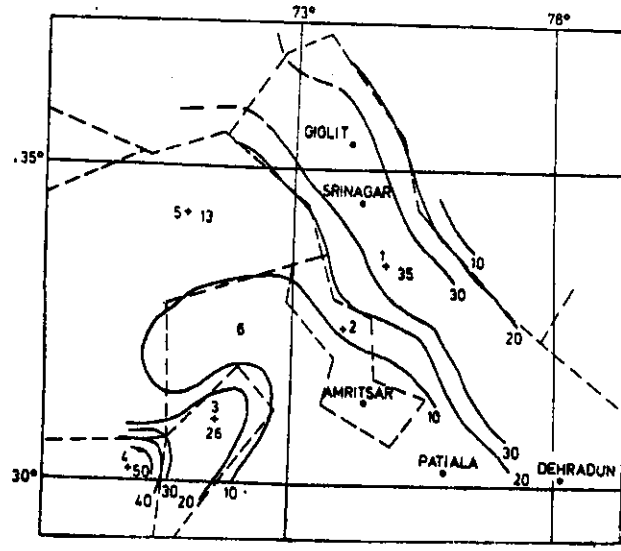

(a)

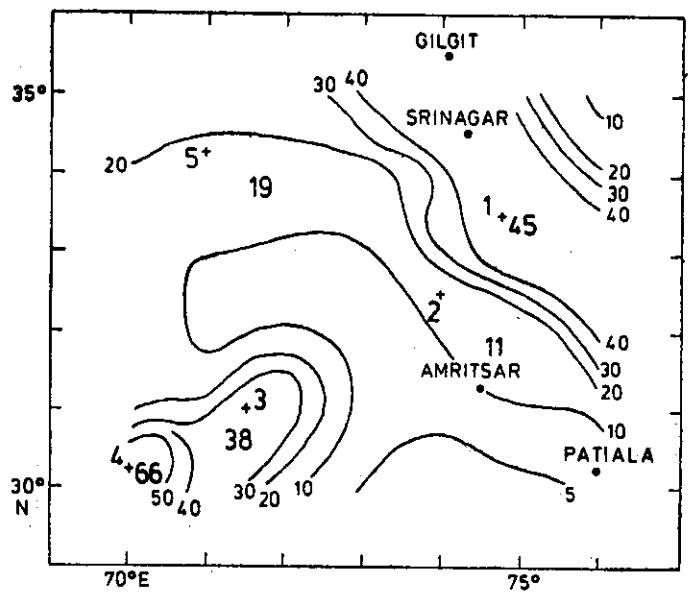

(b)

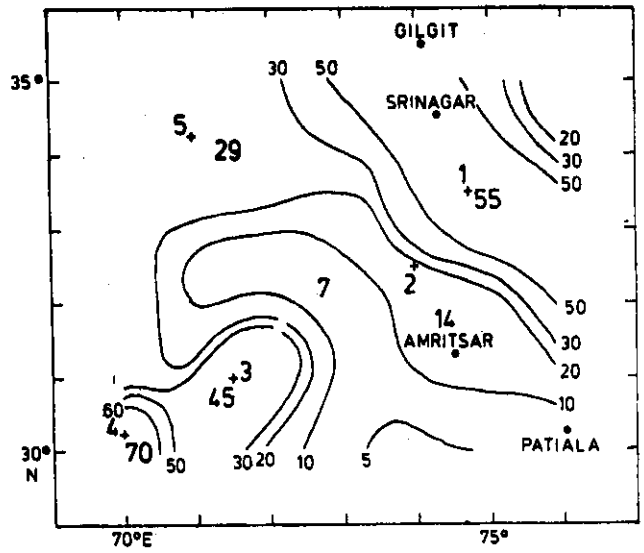

(c)

Fig. 8. Probabilistic seismic hazard maps of the north-west India and neighbourhood. The contours show the maximum peak ground accelerations in percent g that have a 10% probability of exceedence in any given exposure period (a) Exposure period=50 years. (b) Exposure period=100 years. (c) Exposure period=200 years.

Figures 9(a)–(e) show the graphs of the expected peak ground acceleration versus the probability of exceedence, or the return period at five critical locations in the area of investigation. These locations are marked in the hazard maps shown in Figure 8.

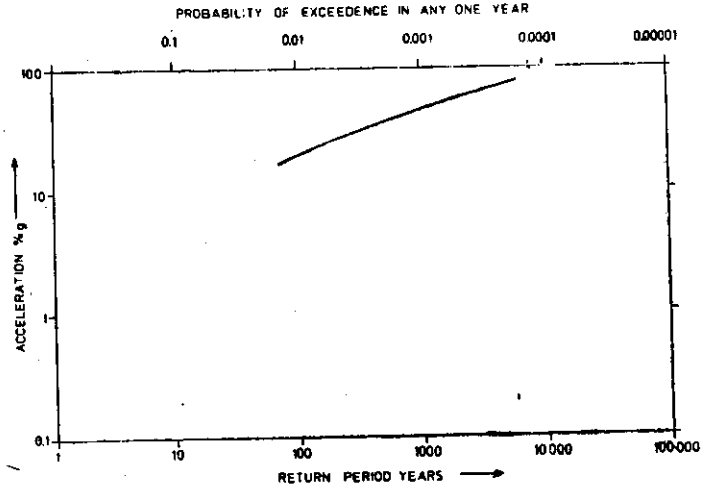

(a)

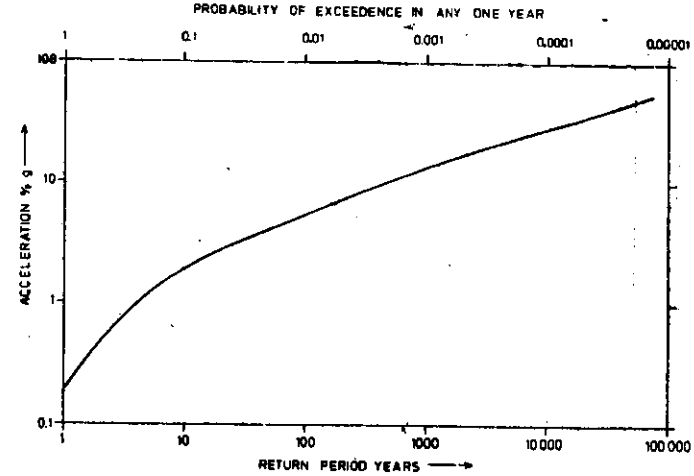
PROBABILITY OF EXCEEDENCE IN ANY ONE YEAR
1
0.1
0.01
0.001
0.0001
0.00001
100
10
1
0.1
ACCELERATION % g
1
10
100
1000
10 000
100 000
RETURN PERIOD YEARS

(b)

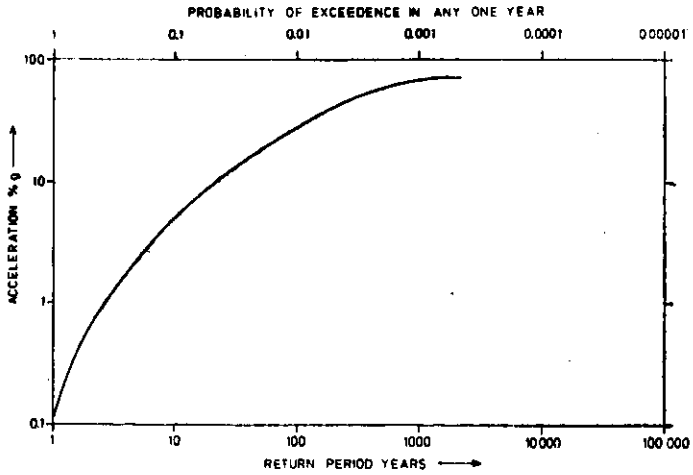
PROBABILITY OF EXCEEDENCE IN ANY ONE YEAR
1
0.1
0.01
0.001
0.0001
0.00001
100
10
1
0.1
ACCELERATION % g
1
10
100
1000
10000
100 000
RETURN PERIOD YEARS

(c)

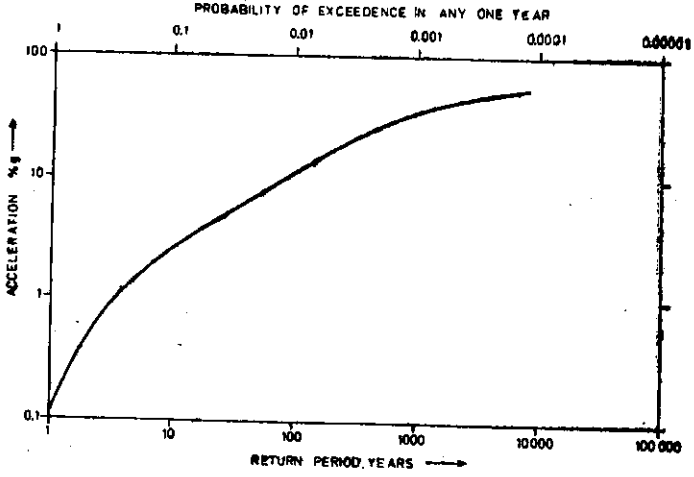
PROBABILITY OF EXCEEDENCE IN ANY ONE YEAR
1
0.1
0.01
0.001
0.0001
0.00001
100
10
1
0.1
ACCELERATION % g
1
10
100
1000
10000
100 000
RETURN PERIOD, YEARS

(d)

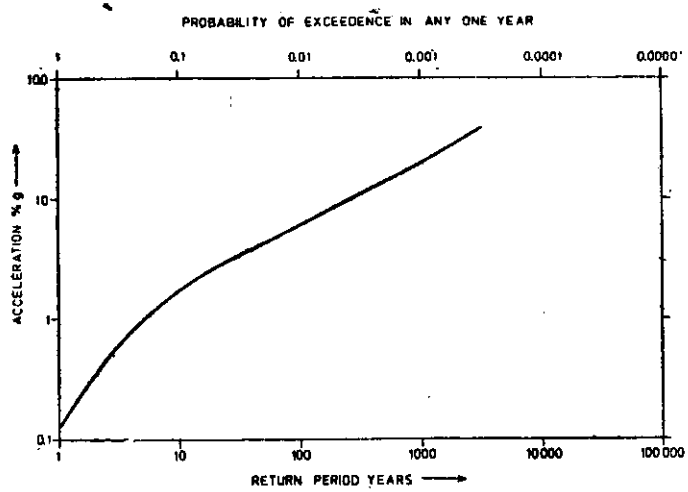

(e)

Fig. 9. The graphs of the peak ground acceleration versus the return period and the probability of exceedence in any one year at locations: (a) 1 (74.75° E, 33.5° N) (b) 2 (74.0° E, 32.5° N); (c) 3 (71.5° E, 31.0°N); (d) 4 (70.0° E, 30.25°N); (e) 5 (71.0° E, 34.25°N). These locations are marked in Fig. 8

It is to be noted that the estimates of the peak ground accelerations obtained are in hard rock. An appropriate scaling would be required for taking into consideration the local site conditions such as the rock type, the geological structure and the topography. The return periods of the accelerations mapped for 50, 100 and 200 year exposure periods respectively are appoximately 475, 950 and 1900 years.

DISCUSSION

The physical processes of the occurence of earthquakes in complex geological environments are as yet poorly understood. As a result the prediction of earthquakes in time, place and magnitude, which would be the best form of earthquake hazard estimate, is an elusive goal. The gross process of the cause of earthquakes is adequately modelled by the elastic rebound theory (Reid, 1910). Under this theory the tectonic strain builds up in rocks over a period of time which is released catastrophically when the rocks fracture to release the accumulated strain and rebound to a position of equilibrium. The release of strain from an earthquake focal region would render it relatively a safer area as the occurrence of future earthquakes would be less likely until the strains are regenerated by the geological processes. Thus the seismicity patterns in an earthquake prone area may vary as a function of time. Such temporal variations have been reported and have been cited as evidence of increased or decreased seismic risk (e.g., Khattri and Wyss, 1978; McCann et al., 1979). The earthquake recurrence process may therefore be more suitably modelled by Markov process (Aki, 1956; Vere-Jones, 1966; Patwardhan et al. 1980). The

use of such models require estimation of more statistical parameters and consequently more adequate data set of earthquakes than is the case for Poisson process. The data sets are inadequate in most regions to permit such analysis beyond estimating average recurrence rates (Cornell, 1968). Moreover, the occurrence of earthquakes has been shown to be not violating the hypothesis of Poisson process if aftershocks and swarms are excluded from the analysis (Wenner, 1937; Niazi, 1964; Lomnitz, 1966: Gardner and Knopoff, 1974). Therefore the use of Poisson model for obtaining first order estimates of the seismic hazard appear to be justified. Similarly until the relative status of the activity of geological faults in the area is known, the uniform distribution of the earthquakes in the source zone is a reasonable alternative. The precision of the hazard maps is also governed by the adequacy of the attenuation distance law. In particular, in the absence of the instrumental records of earthquake strong motion in this region, the absolute level of the peak ground accelerations is not firmly established. Another factor which ought to be taken into consideration is the finite dimension of the earthquake source. The simplest model would be to represent them by line sources. Such line sources could be located where active faults are known from geological investigations. The anticipated influence of such a model would be to raise the seismic hazard level over such faults and to reduce it elsewhere. However, such a line source would be more suitable model of strike slip faults rather than thrust faults.

We note that the peak ground acceleration obtained in the present study in the Himalaya zone are of the same order of magnitude as those displayed by Basu and Nigam (1977) and Basu and Srivastava (1981) in the form of islets in the region under consideration, although their estimates are on the lower side. We believe the estimates presented here are better because of giving consideration to seismotectonic features in defining source zones, making compensation for incompleteness of earthquake catalogs and using more suitable attenuation-distance relationships.

REFERENCES

1. Aki, K. (1956), Some problems in statistical seismology, *Zisin*, 8, 205-228.
2. Algermissen, S.T. and D.M. Perkins (1976), A probabilistic estimate of maximum acceleration in rock in the contiguous United States, *U.S. Goel. Survey, Open-File Report* 76-416, 45 p.
3. Auden, J.B. (1959), Earthquakes in relation to the Damodar Valley Project, *Proc. Ist Symp. Earthquake Engg., Univ. of Roorkee, Roorkee, India.*
4. Auden, J.B. and A.M.N. Ghosh (1934), Preliminary account of the earthquake of the 15th January, 1934, in Bihar and Nepal, *Rec. Geol. Survey India* 68 (2), 177–239.

5. Basu, S. and N.C. Nigam (1977), Seismic risk analysis of Indian Peninsula, *Proc. 6th World Conf. Earthquake Engg., New Delhi, India*, **2**, 425–431.

6. Basu, S. and Nigam, N.C. (1978), On seismic zoning map of India, *6th Symp. Earthquake Engg. Roorkee Univ., Roorkee, Vol.–I*, 83-109.

7. Basu, S. and L.S. Srivastava (1981), Seismic design zoning map of India, *Symp. Earthquake Disaster Mitigation, Roorkee University, Roorkee, Vol. I*, 99–109.

8. Bonilla, M.G. and J.M. Buchanan (1970). Interim report on world wide historic faulting, *U.S. Goel. Survey, Open-File Report*, **32** p.

9. Cornell, C.A. (1968), Engineering seismic risk analysis, *Bull. Seism. Soc. Amer.*, **58**, 1583–1606.

10. Evernden, J.F. (1970), Study of regional seismicity and associated problems *Bull. Seism. Soc. Am.*, **60**, 39–446.

11. Gansser, A. (1964). Geology of the Himalayas, *Interscience Publishers*, London, 289 p.

12. Gaur, V.K. and R.K.S. Chouhan (1968) Quantitative measures of seismicity applied to Indian regions, *Bull. Indian Soc. Earthquake Tech.*, **5**, 63–78.

13. Gardner, J.K. and L. Knopoff (1974), Is the sequence of earthquakes in southern California, with aftershocks removed, Poissonian?, *Bull. Seism. Soc. Amer.*, **64**, 1363–1367.

14. Gee, E.R. (1934), The Dhubri earthquake of the 3rd July, 1930, *Mem. Geol. Surv. India*, **65** (1), 1–106.

15. Guha, S.K. (1962), Seismic regionalization of India. *Proc. 2nd, Symp. Earthquake Engg., Roorkee, India*, 191–207.

16. Gupta, H.K. Hari Narain, B.K. Rastogi and I. Mohan (1969), A study of the Koyna earthquake of December 10, 1967, *Bull. Seism. Soc. Amer.*, **59**, 1149–1162.

17. Gupta, H.K., I. Mohan and H. Narain (1972), The Broach earthquake of March 23, 1970, *Bull. Seism. Soc. Amer.*, **62**, 47–61.

18. Gutenberg, B. and C.F. Richter (1942), Earthquake magnitude, intensity, energy, and acceleration, *Bull. Seism. Soc. Amer.*, **32**, 163–191.

19. Gutenberg, B. and C.F. Richter (1956), Earthquake magnitude, intensity, energy, and acceleration, *Bull. Seism. Soc. Amer.*, **46**, 105–145.

20. Hamilton, W.C. (1964), Statistics in Physical Science, *The Ronald Press Co., New York*, 230 pp.

21. Hattori S. (1979), Seismic risk maps in the world (Maximum acceleration and maximum particle velocity) (II)—Balkan, Middle East, South East Asia, Central America, South America and others, *Bull. Intl. Inst. Seismology and Earthquake Engg.*, **17**, 33–96.

22. Howell, B.F. and T.R. Schultz (1975), Attenuation of modified Mercalli intensity with distance from the epicenter, *Bull. Seism. Soc. Amer.*, **65**, 651–665.

23. ISI (1975) Indian standard recommendation for earthquake resistant design of structures, *Indian Standards Institution, New Delhi*, **15**, 1893–1975.

24. Kaila, K.L., and Rao, M. (1979), Seismic Zoning maps of the Indian sub-continent, *Geophys. Res. Bull.*, **17**, 293–301.

25. Khattri, K. and Wyss, M. (1978), Precursory variation of seismicity rate in the Assam area, India, *Geology*, **6**, 685–688.

26. Khattri, K.N., A.M. Rogers, D.M. Perkins and S.T. Algermissen (1983), A seismic hazard map of India and adjacent areas, under submission.

27. Krishna, J. (1959), Seismic zoning of India, *Proc. Ist, Symp. Earthquake Engg., Univ. of Roorkee, Roorkee, India.*

28. Lomnitz, C. (1966), Statistical Prediction of earthquakes, *Reviews of Geophysics*, **4**, 337–393.

29. McCann, E.R., S.P. Nishenko, L.R. Sykes, and J. Krause (1979), Seismic gaps and plate tectonics: seismic potential for major plate boundaries, *Pageoph*, **117**, 1082.

30. Medvedev, S.V. (1959), Correlation between focal depth of earthquakes and isoseismals, in *Problems in Engg. Seism., no. 2, Akad. Nauk. SSSR Inst. Fiziki Zemli Trudy, 5* (**172**), 94–99.

31. Middlemiss, C.S. (1910), The Kangra earthquake of 4th April 1905, *Mem. Geol. Surv. India*, **38**, 409 p.

32. Milne J. (1911), A catalogue of destructive earthquakes—A.D. 7 to A.D. 1899, *Brit. Assoc. Advan. Sci. Rpt., Portsmouth Meet*, **1911**, *Appendix No.* 1, 649–740.

33. Mithal, R.S. and L.S. Srivastava (1959), Geotectonic position and earthquakes of Gango-Bramhaputra region, *Proc. Ist, Symp, Earthquake Engg., Univ. of Roorkee, Roorkee, India.*

34. Niazi, M. (1964), Seismicity of northern California and western Nevada, *Bull. Seism. Soc. Am.*, **54**, 845–850.

35. Oldham, R.D. (1883), Catalogue of Indian earthquakes, *Mem. Geol. Surv. India*, **19**, 163–215.

36. Oldham, R.D. (1899), Report of the great earthquake of 12th June 1897, *Mem. Geol. Surv. India*, **29**, 1–379.

37. Oldham, R.D. (1926), The Cutch (Kacch) earthquake of 16th June, 1819, with a revision of the great earthquake of 12th June, 1897, *Mem. Geol. Survey of India*, **46**. pp 71–174.

38. Patwardhan, A. S., R.B. Kulkarni, and D. Tocher, (1980), A semi-Markov model for characterising recurrence of great earthquakes, *Bull. Seism. Soc. Am.*, **70**, 323–347.

39. Rao, M.B.R. (1953), A compilation of papers on the Assam earthquake of August 15, 1950, *The Central Board of Geophysics Publication*, **1**, 112 p.

40. Reid, H.F. (1910), The mechanics of the earthquake, The California

Earthquake of April 18, 1906, *Report on the State Investigation Commission, Vol. 2, Carnegie Institution of Washington, Washington, D.C.*

41. Shebalin, N.V. (1959), Determination of focal depth from macroseismic data with consideration of the influence of the low velocity layer, in *Problems in Engineering Seismology, no. 2, Akad. Nauk. SSSR Inst. Fiziki Semli Trudy*, **5 (172)**, 100–113.

42. Singh, S., A.K. Jain, P. Sinha, V.N. Singh and L.S. Srivastava (1976), The Kinnaur earthquake of January 19, 1975: A field report, *Bull. Seism. Soc. Amer.*, **66**, 887–901.

43. Stepp, J.C. (1973), Analysis of completeness of the earthquake sample in the Puget Sound area, in Contributions to Seismic Zoning, (ed. S T. Harding), *No. AA Tech. Rpt. ERL 267–ESL* **30**, *U.S. Dept. of Commerce.*

44. Stuart, M. (1920), The Srimangal earthquake of 8th July 1918. *Mem. Geol. Surv. India*, **46 (1)**, 1–70.

45. Tandon, A.N. (1956), Zones of India liable to earthquake damage, *Ind. J. Met. Geophys*, **10**, 137–146.

46. Vere-Jones, D. (1966), A Markov model for aftershock occurrences, *Pure and Applied Geophysics*, **64**, 31–42.

47. Wenner, E. (1937), Statistics of earthquakes I, and II, *Ger. Geitr. Geophys.*, **50**, 85–99 and 223–228.

48. West, W.D. (1936), Preliminary geological report on the Baluchistan (Quetta) earthquake of May 31, 1935, *Rec. Geol. Surv. India.*, **69 (2)**, 203–240.